

Testing Independence with the Binary Expansion Randomized Ensemble Test

Duyeol Lee¹, Kai Zhang¹, and Michael R. Kosorok^{1,2}

¹Department of Statistics and Operations Research, University of North Carolina, Chapel Hill, NC 27599

²Department of Biostatistics, University of North Carolina, Chapel Hill, NC 27599

June 9, 2022

Abstract

Recently, the binary expansion testing framework was introduced to test the independence of two continuous random variables by utilizing symmetry statistics that are complete sufficient statistics for dependence. We develop a new test by an ensemble method that uses the sum of squared symmetry statistics and distance correlation. Simulation studies suggest that this method improves the power while preserving the clear interpretation of the binary expansion testing. We extend this method to tests of independence of random vectors in arbitrary dimension. By random projections, the proposed binary expansion randomized ensemble test transforms the multivariate independence testing problem into a univariate problem. Simulation studies and data example analyses show that the proposed method provides relatively robust performance compared with existing methods.

Keywords: Nonparametric inference; Nonparametric test of independence; Binary Expansion; Multiple testing; Multivariate analysis.

1 Introduction

Nonparametric testing of independence is a fundamental problem in statistics and has been studied carefully by many classical papers such as [Hoeffding \(1948\)](#). This problem has been gaining greater interest recently due to its important roles in machine learning and big data analysis. Some important recent developments include [Székely et al. \(2007\)](#); [Gretton et al. \(2008\)](#); [Heller et al. \(2012\)](#); [Wang et al. \(2016\)](#); [Pfister et al. \(2018\)](#); [Gorsky and Ma \(2018\)](#); [Ma and Mao \(2019\)](#); [Berrett and Samworth \(2019\)](#). [Josse and Holmes \(2016\)](#) have published an authoritative review.

One important problem in nonparametric dependence detection is nonuniform consistency, which means that no test can uniformly detect all forms of dependency, as described by [Zhang \(2019\)](#). This problem is particularly severe for nonlinear relationships, which are common in many areas of science. To avoid the power loss due to nonuniform consistency, [Zhang \(2019\)](#) considers the binary expansion statistics (BESat) framework; this framework examines dependence with a filtration approach induced by the binary expansion of uniformly distributed variables. [Zhang \(2019\)](#) also proposed testing independence of two continuous variables with the framework of maximum binary expansion testing (BET). The maximum binary expansion testing achieves uniformity and the minimax rate for sample size requirement for desired power. It also provides clear interpretability, and it can be implemented efficiently by bitwise operations.

Although maximum binary expansion testing works well in testing independence between two variables, two crucial improvements are needed for greater practical applicability. The first requirement is to improve the power when the sparsity assumption is violated in Theorem 4.4 of [Zhang \(2019\)](#). The second requirement is to extend the test for testing independence of random vectors. In this paper, we describe a new approach that solves both of these problems. The first problem is

addressed by a novel ensemble approach, and the second problem is solved by using one-dimensional random projecting. Due to random projection and ensemble, we call the new method the binary expansion randomized ensemble test. We show with simulation studies that the proposed method has good power properties, and it maintains the clear interpretability of maximum binary expansion testing.

2 Proposed Method

2.1 The Binary Expansion Testing Framework

We briefly introduce the testing procedure and useful notations from [Zhang \(2019\)](#). Let $(X_1, Y_1), \dots, (X_n, Y_n)$ be a random sample from distributions of X and Y . If the marginal distributions of X and Y are known, we can use the CDF transformation so that $U = F_X(X)$ and $V = F_Y(Y)$ are each uniformly distributed over $[0, 1]$. The binary expansions of two random variables U and V can be expressed as $U = \sum_{k=1}^{\infty} A_k/2^k$ and $V = \sum_{k=1}^{\infty} B_k/2^k$ where $A_k \stackrel{i.i.d.}{\sim} \text{Bernoulli}(1/2)$ and $B_k \stackrel{i.i.d.}{\sim} \text{Bernoulli}(1/2)$. If we truncate the expansions at depth d , then $U_d = \sum_{k=1}^d A_k/2^k$ and $V_d = \sum_{k=1}^d B_k/2^k$ are two discrete variables that can take 2^d possible values. We define the binary variables $\dot{A}_i = 2A_i - 1$ and $\dot{B}_j = 2B_j - 1$ to express the interaction between them as their products. We call the variables of the form $\dot{A}_{k_1,i} \dots \dot{A}_{k_r,i} \dot{B}_{k'_1,i} \dots \dot{B}_{k'_t,i}$ with $r, t > 0$ cross interactions. To explain, we use the following binary integer indexing. Let a be a d -dimensional binary vector with 1's at k_1, \dots, k_r and 0's otherwise, and let b be a d -dimensional binary vector with 1's at k'_1, \dots, k'_t and 0's otherwise. With this notation, the cross interaction $\dot{A}_{k_1} \dots \dot{A}_{k_r} \dot{B}_{k'_1} \dots \dot{B}_{k'_t}$ can be written as $\dot{A}_a \dot{B}_b$.

Next, we denote the sum of the observed binary interaction variables by $S_{(ab)} = \sum_{i=1}^n \dot{A}_{a,i} \dot{B}_{b,i}$ with $S_{(00)} = n$. These statistics are referred to as the symmetry statistics. If U_d and V_d are independent, $(S_{(ab)} + n)/2 \sim \text{Binomial}(n, 1/2)$ for $a \neq 0$

and $b \neq 0$. If marginal distributions are unknown, we can use the empirical CDF transformation and then $(\widehat{S}_{(ab)} + n)/4 \sim \text{Hypergeometric}(n, n/2, n/2)$ where $\widehat{S}_{(ab)}$ is a symmetry statistic with empirical CDF transformation.

The maximum binary expansion testing procedure at depth $d = d_{max}$ can be defined as follows. First, we compute all symmetry statistics with $a \neq 0$ and $b \neq 0$ for $d = d_{max}$. For each depth $d = 1, \dots, d_{max}$, we look for the symmetry statistic with the strongest asymmetry and find its p -value. Finally, we use Bonferroni adjustment to obtain a p -value that considers the family-wise error rate.

The maximum binary expansion testing procedure has several advantages. Let $E_{(ab)}$ denote $E[\dot{A}_a \dot{B}_b]$ and E denote the vector whose entries are all $E_{(ab)}$'s with the first entry $E_{(00)} = 1$. Zhang (2019) showed that for any $\epsilon > 0$, the maximum binary expansion testing with size α requires $n = O(2^{(d_1+d_2)/2}/\delta^2)$ observations to have power $1 - \epsilon$ under the assumption $\|E - (1, 0, \dots, 0)^T\|_\infty \geq \sqrt{d_1 + d_2} 2^{-(d_1+d_2)/4} \|E - (1, 0, \dots, 0)^T\|_2$. This requirement is the optimal rate in Paninski (2008). If the sample size increases at any smaller rate, there exist alternatives for which the power is strictly bounded away from 1. That is, the maximum binary expansion testing approach is minimax in the sample size requirement. The test provides both inferences and clear interpretations. For the maximum binary expansion test, rejection of independence implies that there is at least one significant cross interaction. Thus, we can find a potential dependence structure in the sample by investigating the detected cross interaction.

2.2 Univariate Independence Testing Procedure

Although the maximum binary expansion testing procedure shows good performance in many interesting dependency structures, there is room for improvement. In particular, a test based on the sum of squared symmetry statistics provides better power when the sparsity assumption is violated.

Consider a binary expansion test with specified d_{max} . For each depth $d = 1, \dots, d_{max}$, we can find a set of symmetry statistics $S_{(ab)}$. Let C_d be a set of corresponding ab indices of depth d . Since an interaction has different ab indices for two different d , to avoid confusion, we use the ab of depth d_{max} . For example, when $d_{max} = 2$, $C_1 = \{1010\}$ and $C_2 = \{0101, 0110, 0111, 1001, 1010, 1011, 1101, 1110, 1111\}$. The sets C_d have a nested structure. Now, for each depth d , we introduce the proposed measures of dependence.

Definition 2.1. Let $X \in \mathbb{R}$ and $Y \in \mathbb{R}$ be two random variables. The population measure of dependence is defined as

$$\mathcal{B}_d(X, Y) = \frac{1}{(2^d - 1)^2} \sum_{ab \in C_d} E[\dot{A}_a \dot{B}_b]^2 (d = 1, \dots, d_{max}).$$

Definition 2.2. Let $\{(X_i, Y_i)\}_{i=1}^n$ be a random sample from the joint distribution of (X, Y) . The empirical measure of dependence is defined as

$$\mathcal{B}_{n,d}(\{(X_i, Y_i)\}_{i=1}^n) = \frac{1}{(2^d - 1)^2} \sum_{ab \in C_d} \left(\frac{S_{(ab)}}{n} \right)^2,$$

for each depth $d = 1, \dots, d_{max}$.

The following theorem lists some properties of $\mathcal{B}_d(X, Y)$ and $\mathcal{B}_{n,d}(\{(X_i, Y_i)\}_{i=1}^n)$.

Theorem 2.3. The following properties hold:

- (i) $\mathcal{B}_d(X, Y) = 0$ if and only if U_d and V_d are independent.
- (ii) $0 \leq \mathcal{B}_d(X, Y) \leq 1$.
- (iii) $0 \leq \mathcal{B}_{n,d}(\{(X_i, Y_i)\}_{i=1}^n) \leq 1$.
- (iv) $\mathcal{B}_{n,d}(\{(X_i, Y_i)\}_{i=1}^n)$ converges almost surely to $\mathcal{B}_d(X, Y)$ as $n \rightarrow \infty$.
- (v) If X and Y are independent, then $(2^d - 1)^2 n \mathcal{B}_{n,d}(\{(X_i, Y_i)\}_{i=1}^n)$ converges in distribution to $\chi_{(2^d - 1)^2}^2$ as $n \rightarrow \infty$.

We define the scaled sum of squared symmetry statistics for each depth $d = 1, \dots, d_{max}$ as

$$\xi_d = \sum_{ab \in C_d} \frac{S_{(ab)}^2}{n}. \quad (2.1)$$

By this definition, each ξ_d can be used to detect the dependencies up to depth d . Consider a test that rejects H_0 : X and Y are independent if at least one of ξ_d 's is greater than $\xi_{d,1-\alpha_d}$, the $1 - \alpha_d$ quantile of ξ_d . Then, by Boole's inequality, the upper bound of the type I error is

$$pr(\text{reject } H_0 \mid H_0 \text{ is true}) \leq \sum_{d=1}^{d_{max}} \alpha_d. \quad (2.2)$$

There are many possible versions of the test based on different choices of the α_d 's. Each ξ_d has a corresponding set of alternatives that it performs well. Therefore, if we have prior information about the dependency, we can choose α_d 's in a way that provides optimal power for certain alternatives. When there are no specific prior alternatives, we need a strategy for choosing the α_d 's. We remark here that the alternatives in C_d for smaller d are more interpretable than those for larger d . From this point of view, we propose an exponentially decaying approach for choice of α_d . If we choose $\alpha_d = \alpha \gamma^d / \sum_{d=1}^{d_{max}} \gamma^d$ where $0 < \gamma \leq 1$ then the upper bound of the significance level is

$$pr(\text{reject } H_0 \mid H_0 \text{ is true}) \leq \sum_{d=1}^{d_{max}} \frac{\alpha \gamma^d}{\sum_{d=1}^{d_{max}} \gamma^d} = \alpha, \quad (2.3)$$

guaranteeing a level α test. A natural choice of γ is 1 and the alternatives in each subset, as a group, are equally likely to be detected for $\gamma = 1$;

$$pr(\text{reject } H_0 \mid H_0 \text{ is true}) \leq \sum_{d=1}^{d_{max}} \frac{\alpha}{d_{max}} = \alpha. \quad (2.4)$$

The power of the proposed test can be improved by a compromise between a distance correlation test and multiple testing over interactions. The binary expansion testing framework loses power from the adverse effect of multiplicity control over

depth. This loss of power is particularly severe for linear dependency. See a detailed discussion in Section 1.2 in the Supplementary Material of [Zhang \(2019\)](#). By considering distance correlation combined with the proposed test, we can mitigate this power loss. There is only one interaction in ξ_1 and it relates to the upper halves of u and v and the lower halves, thus, ξ_1 represents a linear relationship. Because the above test is composed of multiple hypothesis tests, the test with ξ_1 can be replaced with the distance correlation test. Because we are using a Bonferroni correction for the critical values, this replacement still maintains the targeted level of the test. We call this approach as ensemble method because it combines two testing methods. The proposed procedure consists of the following steps:

Step 1 : Fix $\alpha_1, \dots, \alpha_{d_{max}}$ with $\sum_{d=1}^{d_{max}} \alpha_d = \alpha$.

Step 2 : Find the p -value for the distance correlation test.

Step 3 : For each $d = 2, \dots, d_{max}$, compute ξ_d .

Step 4 : Reject H_0 if either at least one of ξ_d is greater than $\xi_{d,1-\alpha_d}$ or the p -value for the distance correlation test is less than α_1 .

A critical value for each depth $d \geq 2$ is chosen in a way that the proportion of independent samples for which the null hypothesis is rejected does not exceed α_d . We can use either a permutation approach or the asymptotic distribution given in [Theorem 2.3](#).

2.3 Multivariate Independence Testing Procedure

Thus far, we have discussed the binary expansion test for univariate random variables. In this section, we develop a generalized independence test for random vectors. The generalization can be made by converting the independence of random vectors into

the independence of univariate random variables. The lemma allowing this conversion is stated below and proved in Appendix A.

Lemma 2.4. *Let $X \in \mathbb{R}^p$ and $Y \in \mathbb{R}^q$ be two random vectors. Then X and Y are independent if and only if $s^T X$ and $t^T Y$ are independent for all $s \in \mathbb{R}^p, t \in \mathbb{R}^q$ with $\|s\| = 1$ and $\|t\| = 1$.*

This result shows that, to prove independence of random vectors, it is sufficient to consider independence of arbitrary linear combinations of the components. Therefore, the multivariate independence can be tested by checking all possible combinations of s and t . Because testing all possible combinations cannot be implemented, we consider an approximation of the test by including a finite but reasonably broad number of combinations.

Suppose $X \in \mathbb{R}^p$ and $Y \in \mathbb{R}^q$ are two random vectors. For $s \in \mathbb{R}^p, t \in \mathbb{R}^q$ with $\|s\| = \|t\| = 1$, We define a measure of dependence for the multivariate setting by

$$\mathcal{B}_d(X, Y) = \frac{1}{c_p c_q} \int_{\|t\|=1} \int_{\|s\|=1} \mathcal{B}_d(s^T X, t^T Y) ds dt, \quad (2.5)$$

where $c_p = \frac{2\pi^{p/2}}{\Gamma(p/2)}$ and $c_q = \frac{2\pi^{q/2}}{\Gamma(q/2)}$.

Let $\{(X_i, Y_i)\}_{i=1}^n$ be a random sample from the joint distribution of (X, Y) . The empirical measure of dependence for the multivariate setting is defined by

$$\mathcal{B}_{n,d}(\{(X_i, Y_i)\}_{i=1}^n) = \frac{1}{c_p c_q} \int_{\|t\|=1} \int_{\|s\|=1} \mathcal{B}_{n,d}(\{(s^T X_i, t^T Y_i)\}_{i=1}^n) ds dt. \quad (2.6)$$

Note that $\mathcal{B}_{n,d}(\{(X_i, Y_i)\}_{i=1}^n) = E_{S,T}[\mathcal{B}_{n,d}(\{(S^T X_i, T^T Y_i)\}_{i=1}^n) \mid \{(X_i, Y_i)\}_{i=1}^n]$ where S and T follow uniform distributions on hyper-spheres in \mathbb{R}^p and \mathbb{R}^q respectively. This expectation can be estimated by

$$\widehat{\mathcal{B}}_{n,d}(\{(X_i, Y_i)\}_{i=1}^n) = \frac{1}{m} \sum_{j=1}^m \mathcal{B}_{n,d}(\{(S_j^T X_i, T_j^T Y_i)\}_{i=1}^n), \quad (2.7)$$

where $\{(S_j, T_j)\}_{j=1}^m$ is a random sample generated from uniform distributions on

hyper-spheres in \mathbb{R}^p and \mathbb{R}^q . For each depth $d = 1, \dots, d_{max}$, we define the statistic

$$\zeta_d = n(2^d - 1)^2 \widehat{\mathcal{B}}_{n,d}(X, Y). \quad (2.8)$$

By computing $1 - \alpha$ quantiles of ζ_d , for $d = 1, \dots, d_{max}$, we can consider the test that rejects H_0 : “ X and Y are independent” if at least one ζ_d , for $d = 1, \dots, d_{max}$, is greater than $\zeta_{d,1-\alpha_d}$. If $\sum_{d=1}^{d_{max}} \alpha_d \leq \alpha$, this procedure provides a level α test.

For better performance, under possible linear dependency, we combine this procedure with the distance correlation test as above. If the scales of the elements in the random vectors differ greatly, standardization may be helpful to reduce the number of s and t to be sampled. We use the normal quantile transformation for standardization. The following algorithm summarizes the proposed approach.

Step 1 : Set $\alpha_1, \dots, \alpha_{d_{max}}$ with $\sum_{d=1}^{d_{max}} \alpha_d = \alpha$.

Step 2 : Standardize marginally each element of the random vectors.

Step 3 : Find the p -value for the distance correlation test.

Step 4 : Fix $m \in \mathbb{N}$. Generate random sample s_1, \dots, s_m and t_1, \dots, t_m from uniform distributions on hyper spheres, respectively.

Step 5 : For each $d = 2, \dots, d_{max}$, compute ζ_d .

Step 6 : Reject H_0 if either at least one of ζ_d is greater than $\zeta_{d,1-\alpha_d}$ or the p -value for the distance correlation test is less than α_1 .

We refer to this procedure as binary expansion randomized ensemble testing (BERET) due to its two aspects of random projection and ensemble structure. This method has the following advantages. First, the method achieves robust power by a compromise between the distance correlation test and multiple testing over interactions. The power loss due to multiplicity control over the depth also exists in the

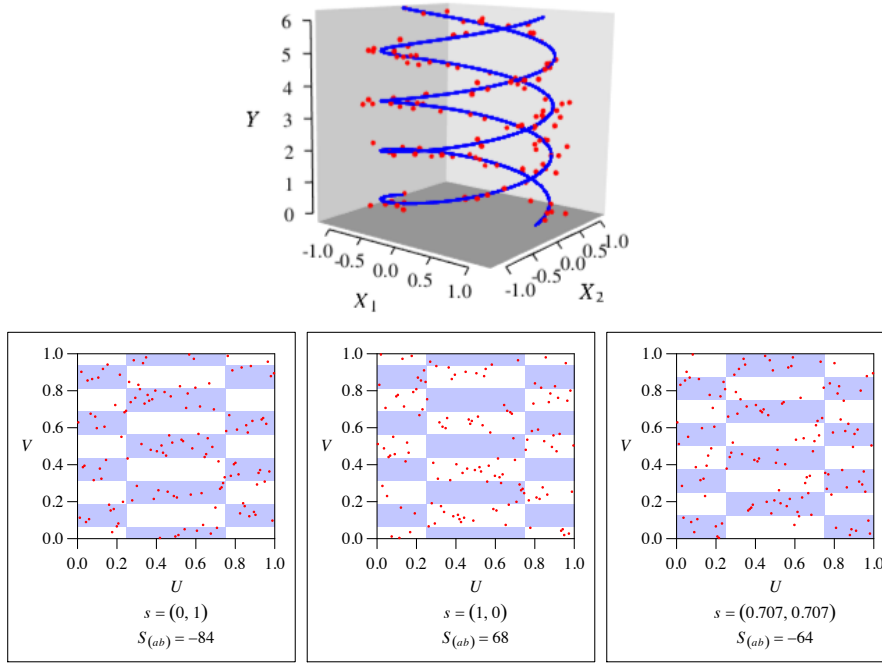


Figure 1: The plot in the first row shows a sample with double helix dependency between a random vector $(X_1 \ X_2)^T$ and a random variable Y with $n = 128$. The blue line is added to illustrate the true relationship. The three plots in the second row show the linear combinations of X_1 and X_2 with the strong asymmetries and the corresponding symmetry statistics ($S_{(ab)}$). Positive regions ($\hat{A}_a \hat{B}_b = 1$) are in white and negative regions ($\hat{A}_a \hat{B}_b = -1$) are in blue.

multivariate case. By considering the distance correlation result together with the proposed measure of dependence with $d \geq 2$, we can improve power over a wide range of plausible dependencies.

The second benefit of our method is clear interpretability. The issue of interpretability is particularly important in evaluating multivariate relationships. However, most multivariate independence tests provide only the results of the tests with no information on potential dependence structures in the sample. Although the canonical correlation test provides some related information, it shows poor power in nonlinear relationships relative to the proposed method. In contrast, when the proposed test rejects independence, the s and t vectors indicate the linear combinations of the vectors that have strong dependencies. Using these vectors, we can detect the possible dependence structures in the sample. See Fig. 1 for a three dimensional double helix

structure example for illustration, in which white positive regions and blue negative regions of interaction provide the interpretation of global dependency. It can be seen that the double helix structure is detected by three linear combinations.

Lastly, our method provides useful exploratory information for model selection. A small entry in the unit vector s or t may indicate that the corresponding variable may not be related to the other random vector. See data examples in Section 4 for details.

3 Simulation Studies

3.1 Univariate Independence

For comparison, we consider the Hoeffding’s D test, the distance correlation test, the k -nearest neighbor mutual information, Fisher’s exact scanning method, and the maximum binary expansion test. We use sample size $n = 128$ as a moderate sample size for power comparison. We set the level of the tests to be 0.1 and simulate each scenario 1,000 times. We adopt $d_{max} = 4$ because this depth provides a good approximation to the true distribution, as mentioned by [Zhang \(2019\)](#). The p-values of the proposed method are calculated using the asymptotic distribution of Theorem 2.3.

We compare the power of the above methods over familiar dependence structures such as linear, parabolic, circular, sine, checkerboard and local relationship described in [Zhang \(2019\)](#). At each noise level $l = 1, \dots, 10$, $\epsilon, \epsilon', \epsilon''$ are independent $\mathcal{N}(0, (l/40)^2)$ random variables. U follows the standard uniform distribution. ϑ is a $U[-\pi, \pi]$ random variable. W, V_1 , and V_2 follow *multi-Bern*($\{1, 2, 3\}, (1/3, 1/3, 1/3)$), *Bern*($\{2, 4\}, (1/2, 1/2)$), and *multi-Bern*($\{1, 3, 5\}, (1/3, 1/3, 1/3)$) respectively. G_1, G_2 are generated from $\mathcal{N}(0, 1/4)$. Table 1 summarizes the details of the setting. Some

graphical descriptions of the scenarios are given in Appendix B.

Scenario	Generation of X	Generation of Y
Linear	$X = U$	$Y = X + 6\epsilon$
Parabolic	$X = U$	$Y = (X - 0.5)^2 + 1.5\epsilon$
Circular	$X = \cos \vartheta + 2\epsilon$	$Y = \sin \vartheta + 2\epsilon'$
Sine	$X = U$	$Y = \sin(4\pi X) + 8\epsilon$
Checkerboard	$X = W + \epsilon$	$Y = \begin{cases} V_1 + 4\epsilon' & \text{if } W = 2 \\ V_2 + 4\epsilon'' & \text{otherwise} \end{cases}$
Local	$X = G_1$	$Y = \begin{cases} X + \epsilon & \text{if } 0 \leq G_1 \leq 1 \text{ and } 0 \leq G_2 \leq 1 \\ G_2 & \text{otherwise} \end{cases}$

Table 1: Simulation scenarios for univariate independence test: linear, parabolic, circular, sine, checkerboard, and local relationships

Figure 2 shows the performance of the six methods. There are two points to notice. First, except for the proposed test, all the other methods show the lowest power in at least one scenario. The ensemble approach and the maximum binary expansion testing show similar powers across the scenarios except for the linear and local dependency. The ensemble approach considerably improves power in the linear and local dependency scenarios. As discussed previously, the ensemble approach utilizes the information on dependence remaining in the symmetry statistics that is not reflected in calculation of the maximum binary expansion testing. Therefore, small asymmetries in many symmetry statistics can be combined to provide a significant result in the ensemble approach when the sparsity assumption is violated. This result is related to the second finding that the ensemble approach outperforms Fisher’s exact scanning in both global and local dependence structures. Zhang (2019) reported that maximum binary expansion testing provides better power for global dependence structures, whereas Fisher’s exact scanning performs better for local dependence structures. The simulation results suggest that the ensemble approach works better than Fisher’s ex-

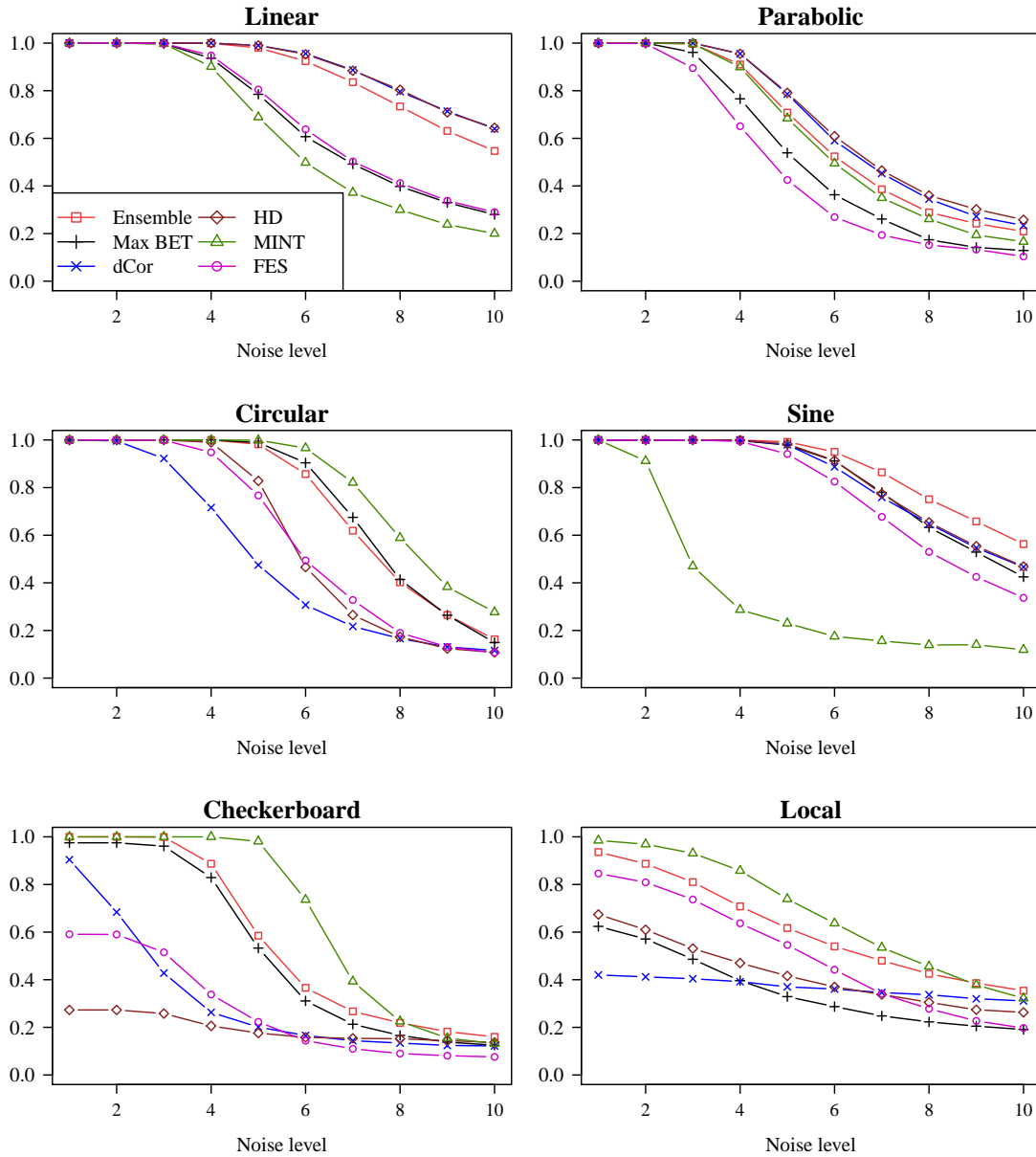


Figure 2: Comparison of powers from six tests of independence: the binary expansion randomized ensemble test with $d_{max} = 4$ (red square), the maximum binary expansion test with $d_{max} = 4$ (black plus sign), the distance correlation test (blue cross), Hoeffding's D (brown diamond), the k -nearest neighbor mutual information (green triangle), and Fisher exact scanning (purple circle).

act scanning even in the local dependency scenario.

3.2 Multivariate Independence

Although the proposed method can be applied to arbitrary p and q , we choose $p = 2$ and $q = 1$ for better illustration. We compare the proposed method with the distance correlation test, the Heller-Heller-Gorfine test, the d -variable Hilbert-Schmidt independence criterion, and the mutual information test. We again use sample size $n = 128$. We set the level of the tests to be 0.1 and simulate each scenario 1,000 times. For our method, we adopt $m = 30$ because there is no considerable difference in performance compared with larger m 's such as $m = 360$. We also use a permutation method with 1,000 replicates to calculate the p-values of the proposed approach.

We compare the power of the methods over dependence structures such as linear, parabolic, spherical, sine, and local dependence structures. These scenarios are generalized from the univariate dependence simulations. In addition, we include an additional interesting relationship, the double helix structure. At each noise level $l = 1, \dots, 10$, $\epsilon, \epsilon', \epsilon''$ are independent $\mathcal{N}(0, (l/40)^2)$ random variables. U_1, U_2 follow the standard uniform distribution. ϑ follows $U[0, 4\pi]$. G_1, G_2, G_3 are independent $\mathcal{N}(0, 1/4)$ random variables. I follow the Rademacher distribution. Table 2 summarizes the details of the setting. These three dimensional scenarios are visually displayed in Appendix B.

Figure 3 shows the simulation results. Our method provides stable results across the scenarios considered. It ranks at least third place in all scenarios. The mutual information test performs best in the highest number of scenarios. It provides the best power in spherical, double helix, and local dependency. In linear and sine relationships, however, there is significant loss of power in the mutual information test compared with the proposed method. The Heller-Heller-Gorfine test is the other test that shows stable performance across all scenarios. It is better than the pro-

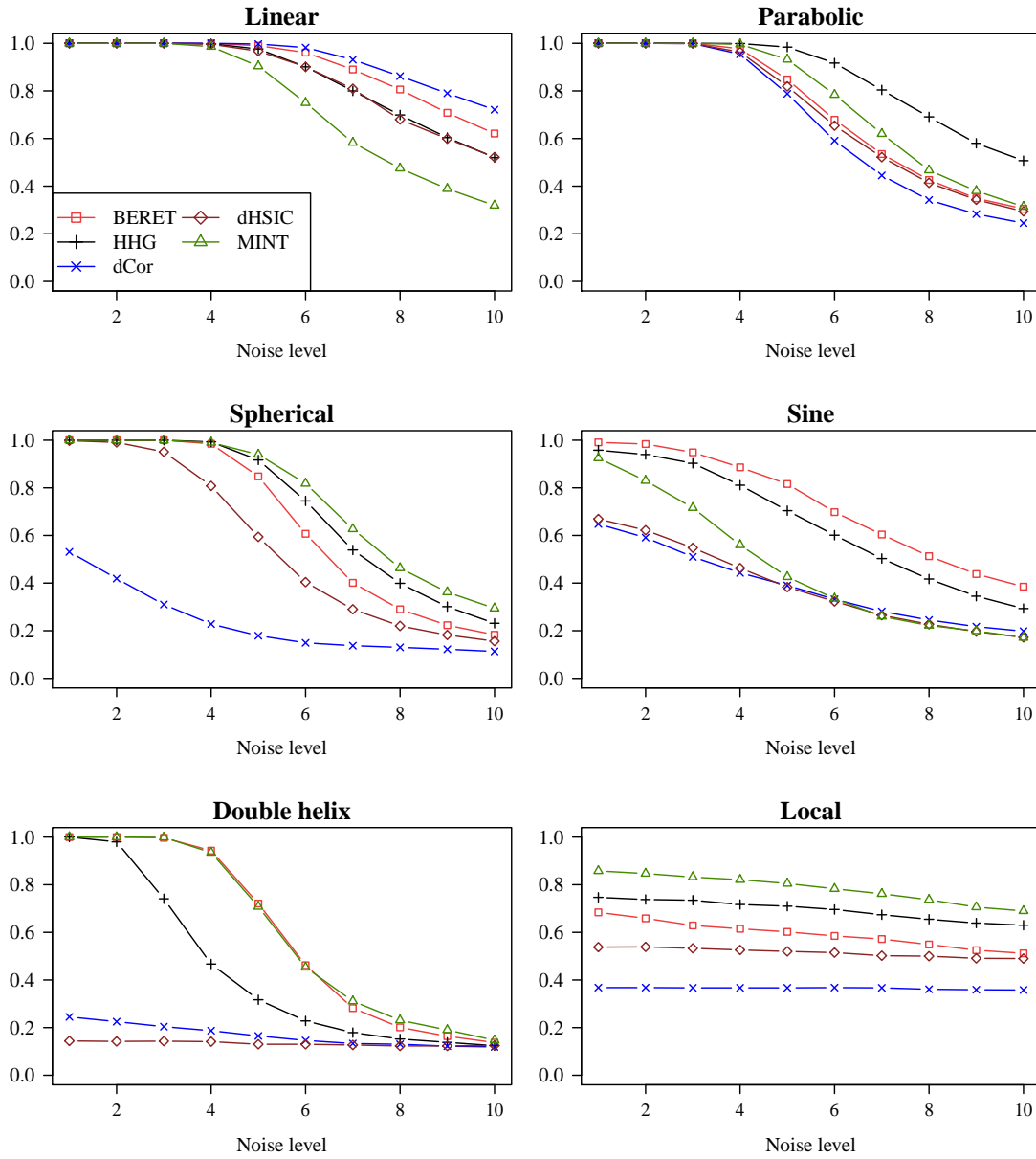


Figure 3: Comparison of powers from five tests of independence: the binary expansion randomized ensemble test with $d_{max} = 4$ (red square), the Heller-Heller-Gorfine test (black plus sign), the distance correlation test (blue cross), the d -variable Hilbert-Schmidt independence criterion (brown diamond), and the mutual information test (green triangle).

Scenario	Generation of X	Generation of Y
Linear	$X = \begin{pmatrix} U_1 \\ U_2 \end{pmatrix}$	$Y = X_1 + X_2 + 7\epsilon$
Parabolic	$X = \begin{pmatrix} U_1 \\ U_2 \end{pmatrix}$	$Y = (X_1 - 0.5)^2 + (X_2 - 0.5)^2 + 1.5\epsilon$
Spherical	$X = \begin{pmatrix} \frac{G_1}{\sqrt{G_1^2 + G_2^2 + G_3^2}} \\ \frac{G_2}{\sqrt{G_1^2 + G_2^2 + G_3^2}} \end{pmatrix}$	$Y = \frac{G_3}{\sqrt{G_1^2 + G_2^2 + G_3^2}} + 3\epsilon$
Sine	$X = \begin{pmatrix} U_1 \\ U_2 \end{pmatrix}$	$Y = \sin(5\pi X_1) + 4\epsilon$
Double helix	$X = \begin{pmatrix} I\cos(\vartheta) + 1.5\epsilon \\ I\sin(\vartheta) + 1.5\epsilon' \end{pmatrix}$	$Y = \frac{\vartheta}{2} + 2\epsilon''$
Local	$X = \begin{pmatrix} G_1 \\ G_2 \end{pmatrix}$	$Y = \begin{cases} \frac{X_1}{\sqrt{2}} + \frac{X_2}{\sqrt{2}} + \frac{\epsilon}{2}, & \text{if } 0 \leq G_1 + G_2 \leq 2 \text{ and } 0 \leq G_3 \leq 1. \\ G_3, & \text{otherwise.} \end{cases}$

Table 2: Simulation scenarios for multivariate independence testing: linear, parabolic, spherical, sine, double helix, and local relationships

posed method in three scenarios and worse in the other three scenarios. That is, our method and the Heller-Hellor-Gorfine test show similar performance. The proposed method outperforms the distance correlation test and the d -variable Hilbert-Schmidt independence criterion in at least five scenarios compared with each testing method separately. A point to notice is that the proposed method provides competitive performance while providing a much clearer interpretation of the dependence structure.

4 Data Examples

4.1 Life Expectancy

We use the proposed method to test independence between geographic location and life expectancy and compare its performance with the performance of other methods,

i.e., the distance correlation test, the Heller-Heller-Gorfine test, the mutual information test, and the canonical correlation test. We include the canonical correlation test because it also provides some information on dependence structure as does the proposed method. For the proposed method, we set $d = 4$ and $m = 30$. The p-value of the test is calculated by a permutation method with 1,000 replicates. The dataset is obtained from the life expectancy report released by the World Health Organization in 2016. The dataset includes males and females and total life expectancy of 189 countries and special administrative regions estimated in 2015. The latitudes (X_1), longitudes (X_2), and total life expectancies (Y) are used in the analysis. Table 3 presents the testing results for the five different methods. All five tests provide p-values close to 0, indicating a significant dependence between geographic location and life expectancy. To identify the dependence structure, we investigate the symmetry statistics. Figure 4 shows the three largest symmetry statistics and the corresponding s 's.

	BERET	dCor	HHG	MINT	CC
Original sample	<0.0001	<0.0001	0.0010	0.0010	<0.0001
With noise	<0.0001	<0.0001	0.0010	0.0010	<0.0001
$n = 64$	0.0020	0.0014	0.0050	0.0010	0.0158
$n = 32$	0.0806	0.0652	0.0877	0.0177	0.0995

Table 3: p-values from five tests of independence. BERET, the binary expansion randomized ensemble test with $d_{max} = 4$; dCor, the distance correlation test; HHG, the Heller-Heller-Gorfine test; MINT, the mutual information test; CC, the canonical correlation test. The values for subsamples and the samples with noise are average p-values from 100 simulations.

The most asymmetric result is shown in the first row. It is $\dot{A}_2\dot{B}_1$ with $s = (0.516, 0.857)^T$. The horizontal axis is the empirical cumulative distribution function transformation of $0.516X_1 + 0.857X_2$, wherein a smaller value implies the country is located in the southeast and a larger value implies the northwest. There are four

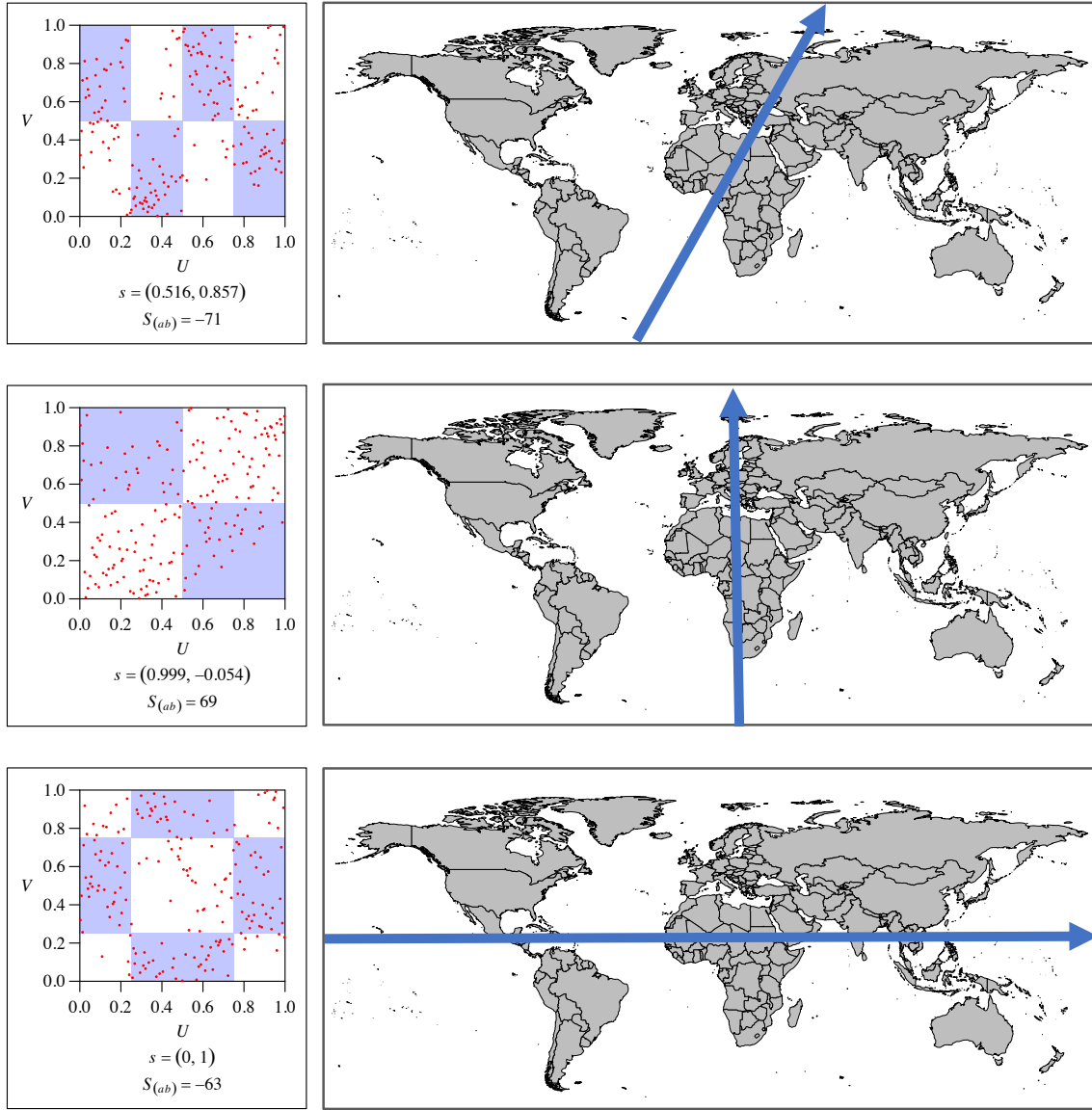


Figure 4: The plots show the three strongest dependency structures between geographic location and life expectancy. They also present the corresponding values of the symmetry statistics ($S_{(ab)}$) and the coefficients of the linear combination (s) of X_1 and X_2 . The blue arrows in the world maps represent the horizontal axes in the scatterplots.

different groups, from the first one in the upper left to the fourth group in the lower right. Each blue cell represents a specific region, America, Africa, Europe and Asia from left to right. The countries in America and Europe show higher life expectancy than countries in Africa and Asia. The four points in the top right corner are Hong Kong, Japan, Macau and South Korea. They can be interpreted as potential outliers distinct from the global pattern.

The second row shows that there is a positive relationship between latitude and life expectancy. That is, the countries in North America, Europe and Northeast Asia have higher life expectancy than countries in Africa, South America and the other parts of Asia. The last row shows that a circular dependency can exist, which indicates that countries in the America and Asia have a medium life expectancy, whereas countries around the prime meridian have different life expectancies, higher in Europe and lower in Africa. These findings prove clearly that our method detects the dependence structures between geographic location and life expectancy.

The canonical correlation analysis also can be used to find information on dependence structure. The canonical correlation is 0.43, and it is calculated using $0.991X_1 - 0.137X_2$ and Y . The coefficients of X_1 and X_2 are similar to the elements of s in the result of the proposed method in the second row. However, canonical correlation provides information only on the linear dependence structure, whereas our method provides richer information by considering various nonlinear dependence structures.

Now we add two randomly sampled noise variables to each X and Y to determine whether the proposed method can identify the pair of subgroups that depend on each other. Each noise variable is chosen from a standard normal distribution. Table 3 presents the p-values for the five different methods. The p-values of all five methods are robust. Figure 5 shows the previously detected strongest dependence structure without noise variables along with an example of the corresponding result with noise

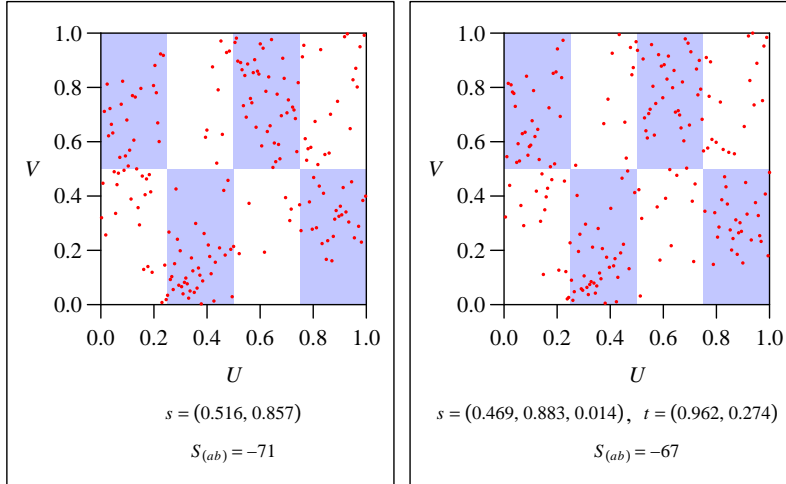


Figure 5: The left plot shows the strongest dependency structures between geographic location and life expectancy. The right plot shows the corresponding result after inclusion of noise variables. The third entry of the vector s and the second entry of the vector t in the right plot are the coefficients of noise variables. The plots also present the values of the symmetry statistics ($S_{(ab)}$) and the coefficients in the linear combinations s and t .

variables. The coefficients of the variables are stable and the coefficients of the noise variables are small.

To compare small sample performance, we randomly selects subsample from the original sample. To mitigate the effect of randomness we calculate the average p-values from 100 simulations. Table 3 displays the average p-values of all five methods. All p-values are similarly affected, and all of them increase as sample size decreases.

In summary, all five methods detects the dependence with very small p-values. In addition, our method detects three interesting dependence structures which can be explained by known global features. The effects of inclusion of noise variables and reduction in sample size are similar for the five methods.

4.2 Mortality Rate

The second case is the relationship between mortality rate, birth rate and income level. We use the Central Intelligence Agency’s world fact data, estimated in 2018.

The dataset includes income level (X_1), birth rate (X_2), and mortality rate (Y) of 225 countries and special administrative regions. Table 4 presents the calculated p-values.

	BERET	dCor	HHG	MINT	CC
Original sample	0.0040	0.0050	0.0010	0.3077	0.4303
With noise	0.0231	0.0213	0.0020	0.3671	0.5272
$n = 64$	0.0287	0.3288	0.1768	0.4998	0.4350
$n = 32$	0.2812	0.4631	0.3304	0.4778	0.4359

Table 4: p-values from five tests of independence. BERET, the binary expansion randomized ensemble test with $d_{max} = 4$; dCor, the distance correlation test; HHG, the Heller-Heller-Gorfine test; MINT, the mutual information test; CC, the canonical correlation test. The values for subsamples and the samples with noise are average p-values from 100 simulations.

Once again, the proposed method and two other methods provide p-values close to 0, which rejects the null hypothesis, whereas the mutual information test and canonical correlation fail to reject it. The poor performance of canonical correlation can be explained by investigating the results of our method. The strongest asymmetry is given in Fig. 6, which shows a strong quadratic relationship. This relationship explains the failure of canonical correlation to work for the data we use here. Although the canonical correlation test provides both inference and information on dependence structure, it performs poorly in nonlinear dependency settings.

For explanation of the observed quadratic relationship one must point to two conflicting phenomena. The first one is that in developed countries the birth rates are low, but the mortality rates are high due to population aging. In developing countries, however, the birth rates are high from lack of family planning and the mortality rates are also high due to insufficient public health. Thus, mortality rates are high in countries with low or high birth rates.

We investigate the effect of noise variable in the same manner. The p-values of five different methods are represented in Table 4, which shows that all five methods

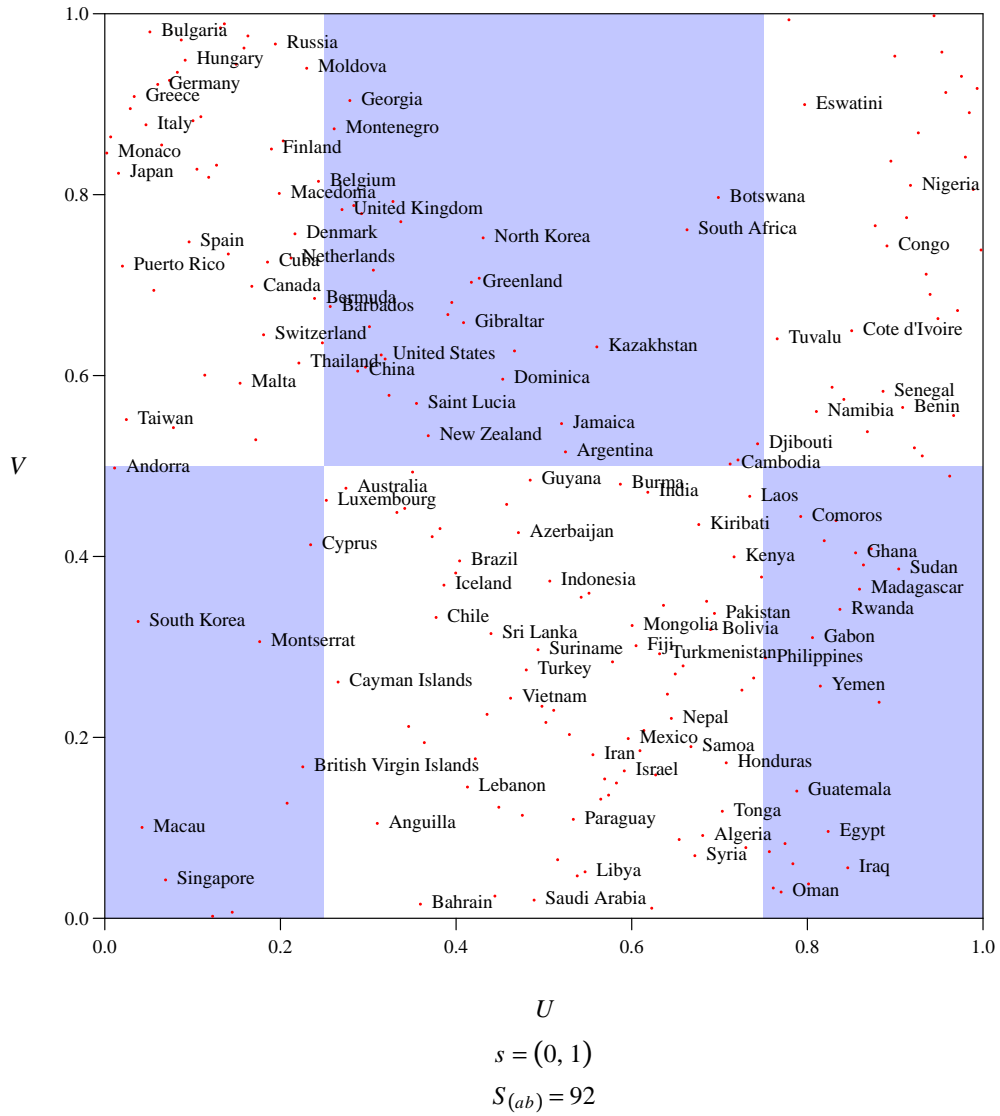


Figure 6: The plot shows the strongest dependency structure between birth rate, income level and mortality rate. It also presents the corresponding value of the symmetry statistic ($S_{(ab)}$) and the coefficients of the linear combination (s) of X_1 and X_2 .

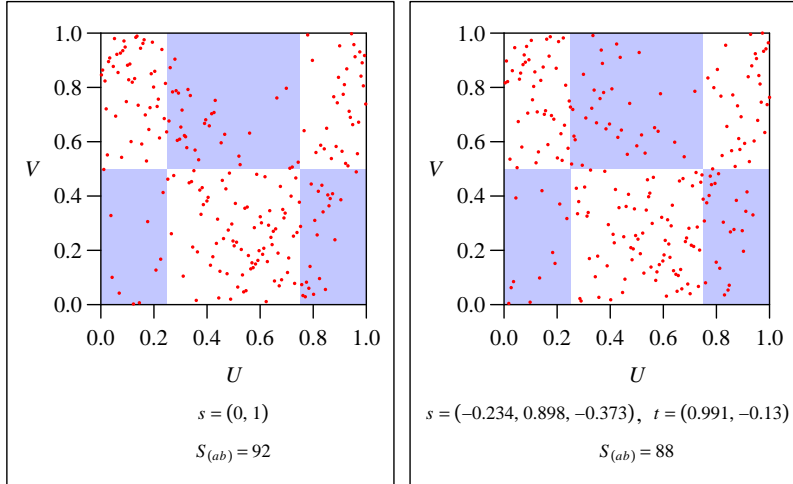


Figure 7: The plots show the strongest dependency structure between birth rate, income level and mortality rate with and without noise variables. The third entry of the vector s and the second entry of the vector t in the right plot are the coefficients of noise variables. The plots also present the values of the symmetry statistics ($S_{(ab)}$) and the coefficients in the linear combinations s and t .

are similarly affected by the noise variables. The strongest dependence structures detected by our method are presented in Fig. 7. The coefficients of noise variables are relatively small, and the same dependence structures are identified as before.

For small sample performance comparison, we randomly selects subsample from the sample as we did in the previous example. Table 4 lists the average p-values. The result shows that the p-values of the distance correlation test and the Heller-Heller-Gorfine test are significantly more affected on average than the p-values of the proposed method.

Once again, the binary expansion randomized ensemble test detects interesting structure that can be explained by widely recognized relationships between mortality rate and birth rate. It provides stable performance even when there are noise variables or when the sample size is small, whereas other methods can be significantly affected by a reduction in sample size.

4.3 House Price

The third data example is the market historical dataset of real estate from the University of California, Irvine machine learning repository. The data includes 414 transactions from the Xindan district of Taipei between August 2012 and July 2013. We use these data to detect the relationship between geographic location and house price. The p-values of the five methods are presented in Table 5.

	BERET	dCor	HHG	MINT	CC
Original sample	<0.0001	<0.0001	0.0010	0.6204	<0.0001
With noise	0.0040	0.4910	0.4961	0.5206	<0.0001
$n = 64$	<0.0001	<0.0001	0.0010	0.2809	<0.0001
$n = 32$	<0.0001	<0.0001	0.0016	0.2660	0.0067

Table 5: p-values from five tests of independence. BERET, the binary expansion randomized ensemble test with $d_{max} = 4$; dCor, the distance correlation test; HHG, the Heller-Heller-Gorfine test; MINT, the mutual information test; CC, the canonical correlation test. The values for subsamples and the samples with noise are average p-values from 100 simulations.

All methods except the mutual information test provide p-values close to 0, which is consistent with the commonly assumed relationship between location and house price in a city. The mutual information test fails to reject the independence. Figure 8 presents the two strongest dependencies identified by the proposed method.

The symmetry statistic with the strongest asymmetry is $\dot{A}_1\dot{B}_1$, which means that there may be a linear relationship between geographic location and house price. The corresponding s for the horizontal axis is $(0.964, 0.268)$. That is, houses have higher values in the north and lower values in the south. It is because the central part of Taipei is above the Xindan district. The symmetry statistic with the second strongest asymmetry is $\dot{A}_1\dot{A}_2\dot{B}_1$. The corresponding s for the horizontal axis is $(0.215, 0.977)^T$. That is, house prices are high at the centre of the district, where two main roads intersect, and prices fall towards the periphery. These results accord closely with

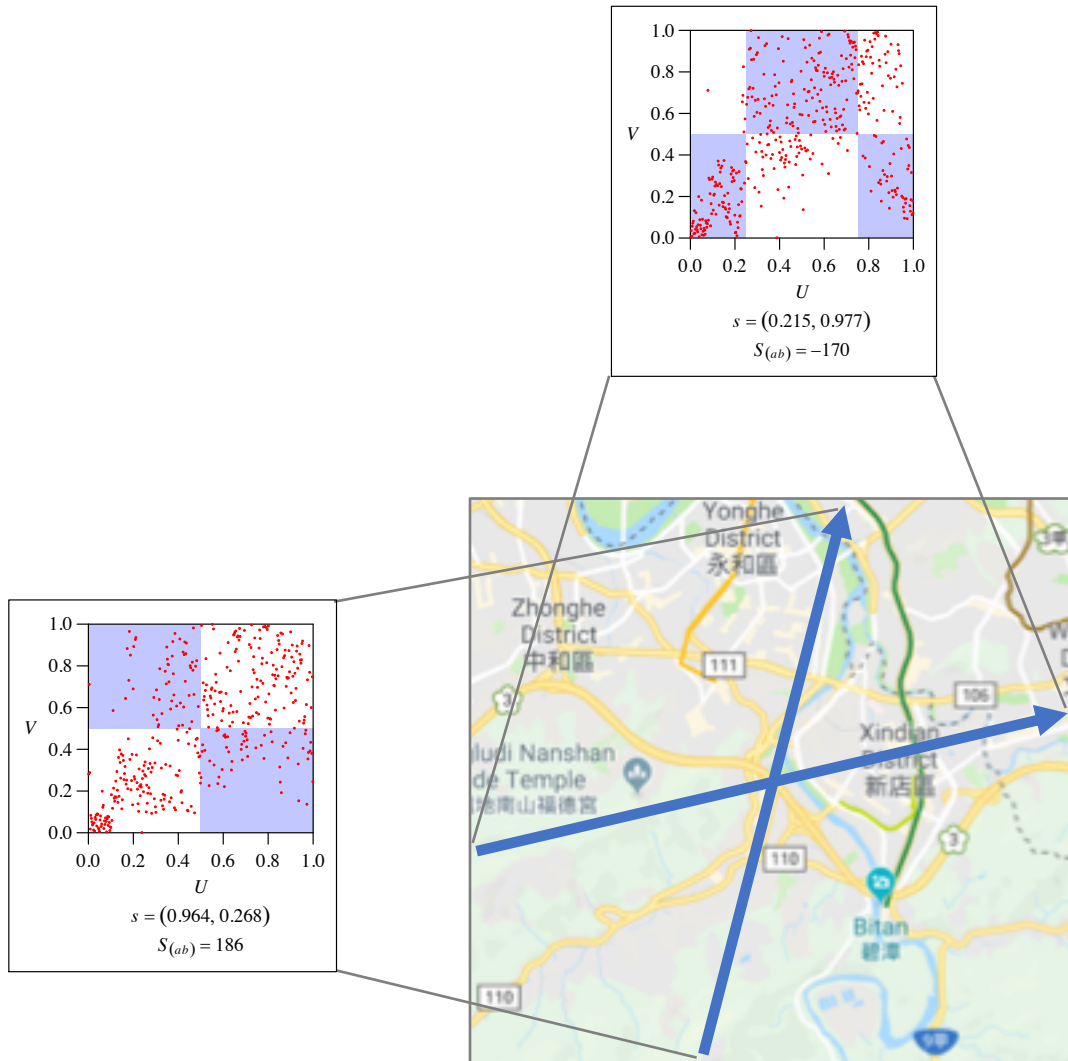


Figure 8: The plots show the two strongest dependency structures between geographic location and house price. The plots also present the values of the symmetry statistics ($S_{(ab)}$) and the coefficients in the linear combinations s and t . The blue arrows in the map represent the horizontal axes in the scatterplots.

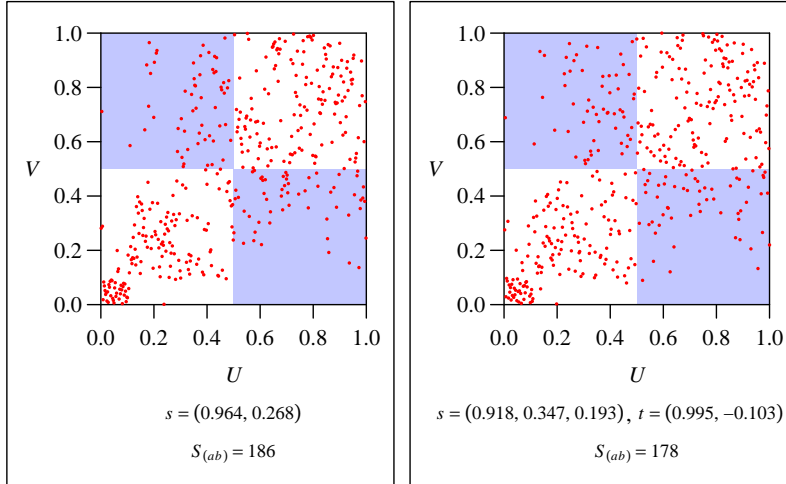


Figure 9: The plots show the strongest dependency structure between geographic location and house price detected by the proposed method without noise variables and the corresponding result with noise variables. The third entry of the vector s and the second entry of the vector t in the right plot are the coefficients of the noise variables. The plots also present the values of the symmetry statistics ($S_{(ab)}$) and the coefficients in the linear combinations s of X_1 , X_2 , and X_3 and t of Y_1 and Y_2 .

the general characteristics of real estate prices in a city. Therefore, we can conclude that the proposed method properly detects the relationships between house price and geographic location.

We add two randomly sampled noise variables to each X and Y as before. The resulting p-values of the five different methods are represented in Table 5. The results of all methods except our method are significantly affected by the noise variables. The detected possible dependence structures by our method are presented in Fig. 9. The figure indicates that the same dependence structures are detected and the coefficients of the noise variables are relatively small as before. The average p-values from the random smaller sample size are also given in Table 5. The result shows that there is little difference in power among the four significant methods.

In conclusion, the proposed method detects the general behavior of house price in the city. The analysis also shows that our method is less affected by noise variables and a decrease in sample size.

5 Discussion

Detection of dependence in a distribution-free setting is an important problem in statistics. Existing methods may have challenges with detecting complicated dependence structures. The distance correlation test, for example, does not detect circular dependency well, whereas it provides good powers in linear, parabolic, and sine settings in simulation studies. The maximum binary expansion testing procedure in [Zhang \(2019\)](#) suggests a novel way to solve this problem. However, it is limited to the independence test of two random variables and there is room for enhancement of power when the sparsity assumption is violated.

In this paper, we introduce an ensemble approach and a binary expansion randomized ensemble test. The ensemble approach uses both the sum of squared symmetric statistics and the distance correlation test. It shows better power in linear and local settings while maintaining power for other dependence structures. Moreover, it can be easily generalized to an independence test for the multivariate setting, the binary expansion randomized ensemble test. By random projections, our method transforms the multivariate independence testing problem into a univariate testing problem. Our approach also maintains the clear interpretability of the maximum binary expansion testing.

Simulation studies suggest that the power of our method is advantageous compared with a range of competitors considered in many meaningful dependence structures. Investigation of three data examples shows that our proposed method reveals hidden dependence structures from the data while maintaining a level of power similar to the best of the competing methods. In addition, the performance of the method is relatively less affected by the existence of noise variables and a decrease in sample size.

Acknowledgement

The authors thank the helpful comments and suggestions from Xiao-Li Meng and Li Ma. This research was partially supported by the National Science Foundation and a grant from the National Cancer Institute.

Appendix A

Proof of Theorem 2.3

- (i) Suppose that $\mathcal{B}_d(X, Y) = 0$. Then $E[\dot{A}_a \dot{B}_b]^2 \leq (2^d - 1)^2 \mathcal{B}_d(X, Y) = 0$ for $a \neq 0$ and $b \neq 0$. If $E[\dot{A}_a \dot{B}_b] = 0$ for $a \neq 0$ and $b \neq 0$, then by definition, $\mathcal{B}_d(X, Y) = 0$. Thus, by Theorem 4.1 in Zhang (2019), $\mathcal{B}_d(X, Y) = 0$ if and only if U_d and V_d are independent.
- (ii) Since $E[\dot{A}_a \dot{B}_b] = 2P(\dot{A}_a \dot{B}_b = 1) - 1$, we have $0 \leq E[\dot{A}_a \dot{B}_b]^2 \leq 1$ and Therefore, $0 \leq \sum_{ab \in C_d} E[\dot{A}_a \dot{B}_b]^2 \leq (2^d - 1)^2$.
- (iii) By the definition of $S_{(ab)}$, we obtain $0 \leq (S_{(ab)}/n)^2 \leq 1$. Since $|C_d| = (2^d - 1)^2$, we have $0 \leq \sum_{ab \in C_d} (S_{(ab)}/n)^2 \leq (2^d - 1)^2$.
- (iv) By the law of large numbers, $S_{(ab)}/n$ converges almost surely to $E[\dot{A}_a \dot{B}_b]$ for $a \neq 0$ and $b \neq 0$. Hence, the conclusion follows at once by the continuous mapping theorem.
- (v) Let S be a vector with entries the $S_{(ab)}$'s. Each $S_{(ab)}/n$ is a sample mean of $\dot{A}_a \dot{B}_b$ terms with mean 0 and variance 1. Since the $S_{(ab)}$'s are pairwise independent, by the central limit theorem, S/\sqrt{n} converges to $\mathcal{N}(0, I_{(2^d-1)^2})$. By the continuous mapping theorem, each $(2^d - 1)^2 n \mathcal{B}_{n,d}(\{(X_i, Y_i)\}_{i=1}^n)$ is asymptotically χ^2 with $(2^d - 1)^2$ degree of freedom.

Proof of Lemma 2.4. Since $a^T X \perp b^T Y$ for all $a \in \mathbb{R}^p, b \in \mathbb{R}^q$ such that $\|a\| = 1$ and $\|b\| = 1$, we have

$$\begin{aligned}
E\left[e^{is(a_1X_1+\dots+a_pX_p)+it(b_1Y_1+\dots+b_qY_q)}\right] &= \phi_{a^T X, b^T Y}(s, t) \\
&= \phi_{a^T X}(s)\phi_{b^T Y}(t) \\
&= E\left[e^{is(a_1X_1+\dots+a_pX_p)}\right]E\left[e^{it(b_1Y_1+\dots+b_qY_q)}\right]
\end{aligned}$$

for all $a \in \mathbb{R}^p, b \in \mathbb{R}^q$ such that $\|a\| = 1$ and $\|b\| = 1$. Now, consider the characteristic function of X and Y . Then, by the above result, we obtain

$$\begin{aligned}
\phi_{X,Y}(s, t) &= E\left[e^{is^T X + it^T Y}\right] \\
&= E\left[e^{i\|s\|\left(\frac{s_1}{\|s\|}X_1+\dots+\frac{s_p}{\|s\|}X_p\right)+i\|t\|\left(\frac{t_1}{\|t\|}Y_1+\dots+\frac{t_q}{\|t\|}Y_q\right)}\right] \\
&= E\left[e^{i\|s\|\left(\frac{s_1}{\|s\|}X_1+\dots+\frac{s_p}{\|s\|}X_p\right)}\right]E\left[e^{i\|t\|\left(\frac{t_1}{\|t\|}Y_1+\dots+\frac{t_q}{\|t\|}Y_q\right)}\right] \\
&= E\left[e^{is^T X}\right]E\left[e^{it^T Y}\right] \\
&= \phi_X(s)\phi_Y(t).
\end{aligned}$$

The opposite direction can also be easily shown.

Appendix B

Fig. 10. displays some examples of the scenarios in the simulation studies of univariate dependence.

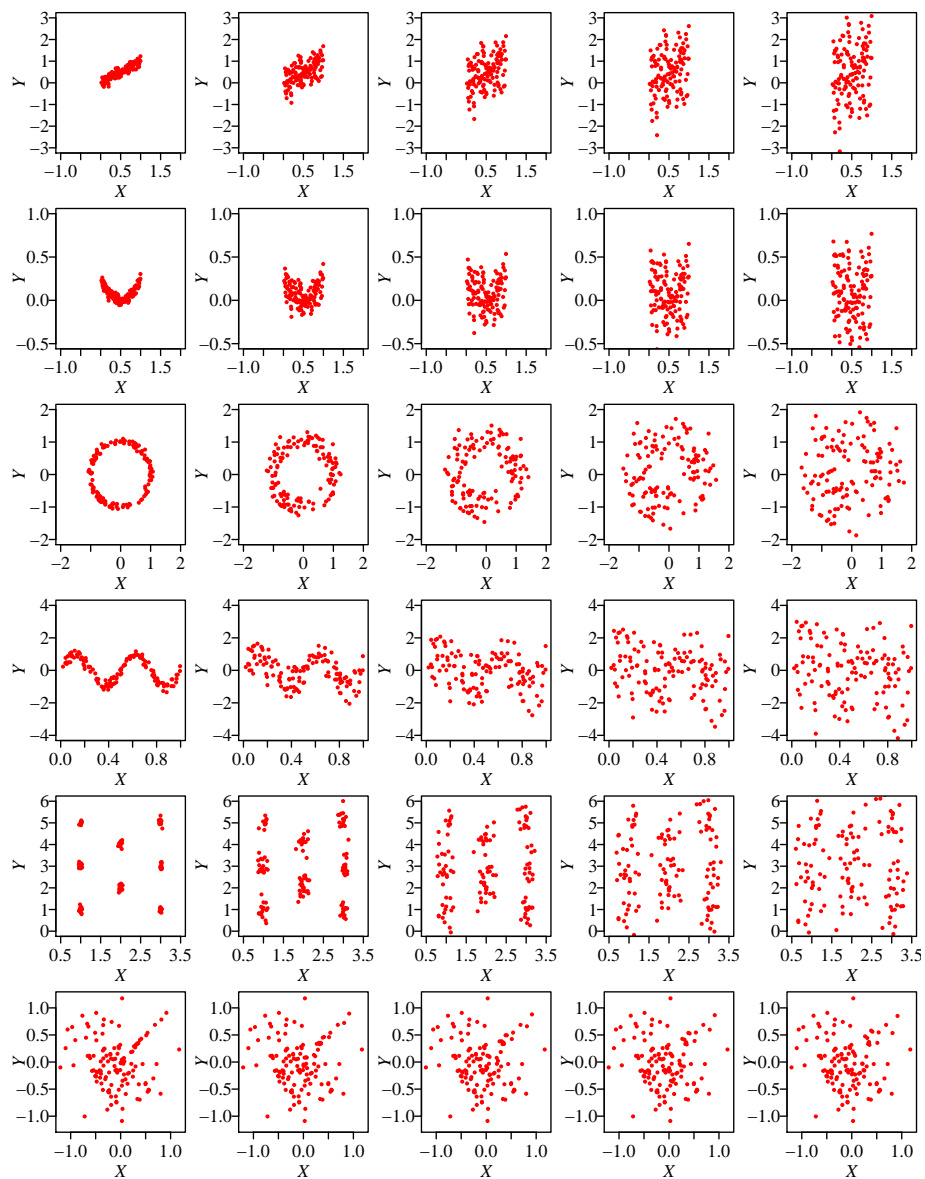


Figure 10: The observations are generated from the six scenarios in Table 1 with $n = 128$ and noise levels $l = 1, 3, 5, 7,$ and 9 . Each row shows the scatterplots of linear, parabolic, circular, sine, checkerboard, and local dependency scenarios in order.

Fig. 11 displays three-dimensional scenarios with sample size $n = 128$. The lowest noise level ($l = 1$) is chosen for better illustration.

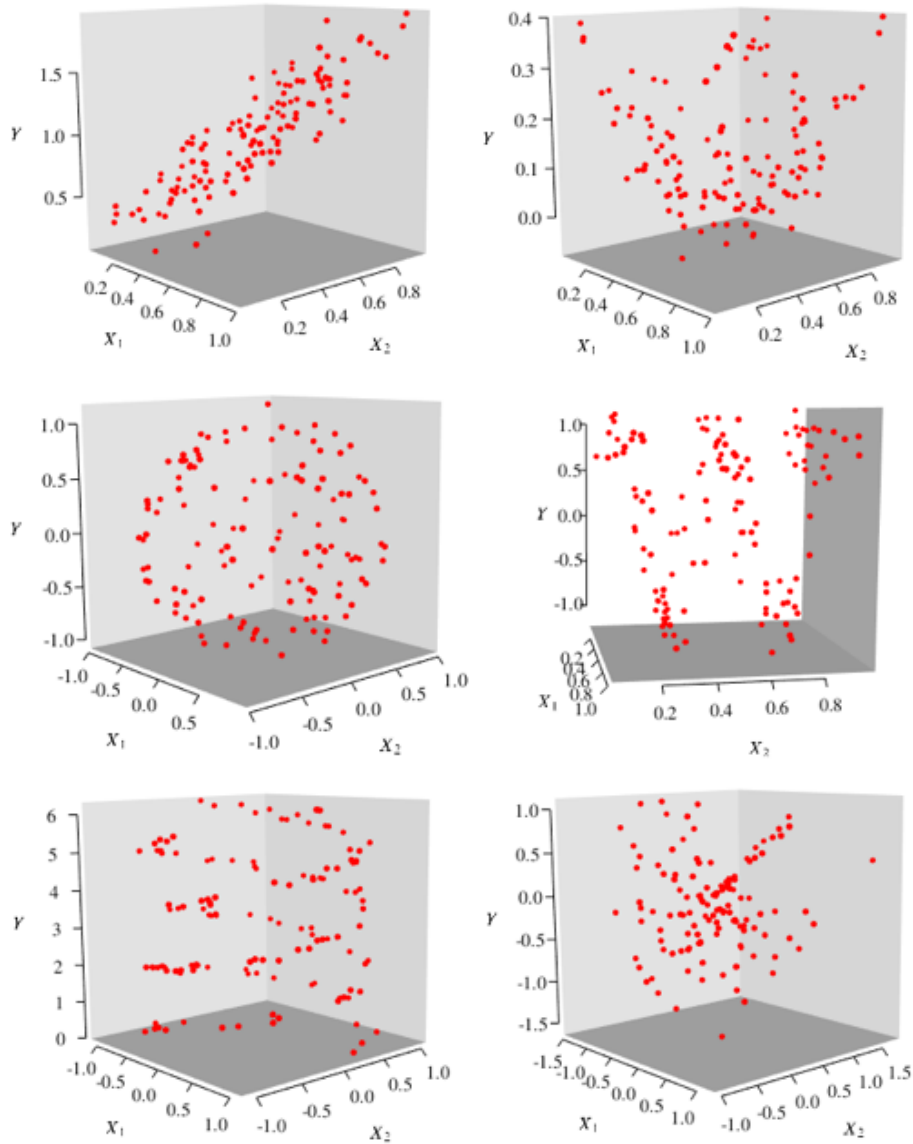


Figure 11: The observations are generated from the six scenarios in Table 2 with $n = 128$ and noise level $l = 1$. Each plot shows the scatterplots of linear (upper left), parabolic (upper right), spherical (middle left), sine (middle right), double helix (bottom left), and local dependency scenarios (bottom right).

References

- Berrett, T. B. and R. J. Samworth (2019). Nonparametric independence testing via mutual information. *Biometrika* 106(3), 547–566.
- Gorsky, S. and L. Ma (2018). Multifit: A multivariate multiscale framework for independence tests. *arXiv:1806.06777*.
- Gretton, A., K. Fukumizu, C. H. Teo, L. Song, B. Schölkopf, and A. J. Smola (2008). A kernel statistical test of independence. In *Advances in neural information processing systems*, pp. 585–592.
- Heller, R., Y. Heller, and M. Gorfine (2012). A consistent multivariate test of association based on ranks of distances. *Biometrika* 100(2), 503–510.
- Hoeffding, W. (1948). A non-parametric test of independence. *Ann. Math. Statist.*, 546–557.
- Josse, J. and S. Holmes (2016). Measuring multivariate association and beyond. *Statist. Surveys* 10, 132.
- Ma, L. and J. Mao (2019). Fisher exact scanning for dependency. *J. Am. Statist. Assoc.*, *accepted*.
- Paninski, L. (2008). A coincidence-based test for uniformity given very sparsely sampled discrete data. *IEEE Transactions on Information Theory* 54(10), 4750–4755.
- Pfister, N., P. Bühlmann, B. Schölkopf, and J. Peters (2018). Kernel-based tests for joint independence. *J. R. Statist. Soc. B* 80(1), 5–31.
- Székely, G. J., M. L. Rizzo, N. K. Bakirov, et al. (2007). Measuring and testing dependence by correlation of distances. *Ann. Statist.* 35(6), 2769–2794.

Wang, X., B. Jiang, and J. S. Liu (2016). Generalized r-squared for detecting non-independence. *arXiv:1604.02736*.

Zhang, K. (2019). Bet on independence. *J. Am. Statist. Assoc.*, to appear. *arXiv:1610.05246*.